

Local Bubble-Size Distribution in Fluidized Beds

D. Santana and A. Macías-Machín

Grupo Energía y Medio Ambiente (EMA) ETSII de Las Palmas, Universidad de Las Palmas de Gran Canaria, Las Palmas de Gran Canaria, Canary Islands 35017 Spain

The importance of the rise angle of bubbles on the influence of local bubble-size distribution in fluidized beds was studied. A new method is proposed for transforming chord-length distribution to a local bubble-size distribution, including the effect of the velocity vector direction on the transformation. Monte-Carlo simulation was used to generate bubbles synthetically with several rise angles, based on the fact that the velocity vector direction distribution of bubbles was a Bingham distribution. The transformation of chord-length data obtained by an imaginary probe, using the Parzen window as an estimation of the probability density function, gives a good estimation of the local bubble-size distribution for different rise angles and the new approach offered here, knowing that the direction of the velocity vector direction for any orientation of the bubbles in the fluidized bed gives a superior agreement than the approach where the local bubble-size distribution is estimated from bubbles with vertical rises.

Introduction

The precise knowledge of the size distribution of bubbles in fluidized beds is an important parameter which is essential to be known. The necessary information to determine energy and mass-transfer processes is obtained from its knowledge. In addition, it is important for an efficient design of fluidized-bed distributors and aerosol generators using a fluidized bed (Henriquez et al., 1995).

The formation and distribution of bubbles in gas fluidized beds greatly influences gas-phase mixing and the circulation patterns of solid particles, which in turn affects the process of attrition and elutriation. The formation of bubbles also has a predominant influence on fluidized beds if this process is used as a method of particle generation (Santana et al., 1999).

Many experimental techniques have been used to determine bubble sizes in fluidized beds such as X-rays, laser electromagnetic and acoustic waves transmissions capacitance probes, optics, densimeters, and pressure probes. A revision of these techniques and their advantages and disadvantages can be found in Cheremisinoff's revision (1986).

From these techniques used to determine the distribution of bubble size, we must take into account that it is impossible to get the bubble size directly from the last four. Instead, we get the distance covered by the probe in the bubble for bub-

bles with a purely vertical rise, from which the size distribution of vertically rising bubbles is inferred.

Therefore, it is important to bear in mind the dependence between the bubble size and the rise angle of bubbles in fluidized beds in the determination of bubble-size distribution.

With regard to the interpretation of pressure signs, an advanced stage of development has been obtained in the later years, mainly with the works of Venkata Ramayya et al. (1996) who have refined both the interpretation of pressure signs in fluidized beds and the determination of the distance measured by the probe when a bubble with vertical rise goes through it.

Recently, Venkata Ramayya et al. (1998) used the differential horizontal pressure to determine if the rise of the bubble is vertical. After that, the problem to determine the bubble-size distribution from the chord lengths read by probes has been proposed. Turton and Clark (1989) solved the problem of inferring the size distribution from the distribution of the probe measurements for the case in which bubbles rise vertically. They have determined the equation which had to verify the probability function of the chord length read by probes and the relationship with the density function of bubble sizes, using the backward numerical transformation from the distance read by the probe.

Liu et al. (1996) and Clark et al. (1996) solved the problem of instability of the backward numerical transformation by

Correspondence concerning this article should be addressed to A. Macías-Machín.

introducing the direct transformation of the distribution of the chord length read by the probe into the bubble-size distribution by means of a nonparametric estimation known as the Parzen's window (Parzen, 1962).

The bubble shape form in the probabilistic analysis is still not solved, except in the areas of bubble size where it is found that the symmetrical ellipsoidal model is a good representation of the process according to Liu et al. (1996).

However, for vertically rising bubbles, there exist several methods for the deduction of bubble-size distribution from a set of chord-length data, but in the case that rise velocity follows intricate directions, it is necessary to know of the attack angle distribution, and there are not experimental data in three-dimensional (3-D) beds. In the case of 2-D beds, Gunn and Al-Doori (1985) and Lim and Agarwal (1992) ascertained the attack angle distribution in 2-D beds by means of an image analysis. However, the hydrodynamic conditions in 2-D beds cannot be compared with the conditions in 3-D beds where the distribution of bubble sizes inside of the bed are not visible.

As a result of the development of the previous work, it is essential to solve the problem for the most realistic case, in which the bubble rise is not necessarily vertical, that is to say, when bubbles have a distribution of velocity vectors. Lim and Agarwal (1992), from observations made on 2-D beds show that the rising bubbles follow an intricate pattern, influenced by other bubbles in the vicinity as well as the local solid flow. These authors have observed that the distribution of bubbles with vertical rises underestimates the smaller bubbles and overestimates the bigger ones.

The objective of this article is to propose a new method for transforming chord-length data to a local bubble-size distribution knowing the direction of the velocity vector because we have considered that the bubbles follow an intricate pattern and bubble orientation and rise velocity may not be vertical. The bubble-shape model employed in this article is the ellipsoidally shaped bubble model, and we have eliminated the errors which could be made when estimating bubble-size distribution by means of readings obtained by probes that only consider the bubble rises vertically.

Analysis of the Probability Relationships

Consider that a submersible probe is operated in a homogeneously bubbling fluidized bed where a swarm of gas bubbles is moving through dense phase medium around the probe. This probe usually measures chord lengths that can be used to characterize bubble sizes. From a distribution of chord lengths, Werther (1974) deduced the bubble-size distribution, by assuming that the bubble shape could be approximated by an ellipsoid.

In our case, in order to determine the bubble-size distribution, the process will be to determine chord length distribution measured by the probe, supposing that the distribution of radii and bubble velocity vectors are known. Then, by means of the analytic backward transform, it is possible to determine the radii distribution once the chord length distribution measured by probes is known.

In Figure 1, we can observe the coordinates system and the dimensions used to determine the density functions and the geometric relationship. The bubble shape model employed in

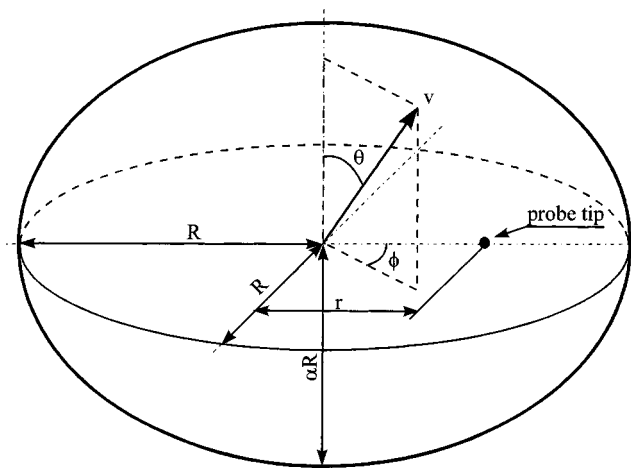


Figure 1. Ellipsoidally shaped bubble model.

this article is the ellipsoidally-shaped bubble model where R is the radius of the bubble, v is the bubble velocity, r stands for the distance between the bubble center and the probe tip, θ is the zenith angle, ϕ is the azimuth angle, and α is a shape factor given by the ratio of the minor (vertical) axis two the major (horizontal) axes, as shown in Figure 1.

Knowing that the bubbles touch the probe, the bubble radius, and the direction of velocity vector, the maximum distance between the center of the bubble and the probe tip is represented by

$$r_{\max} = R \sqrt{\frac{(\alpha \cdot \tan \theta)^2 + 1}{(\alpha \cdot \tan \theta \cdot \sin \phi)^2 + 1}} \quad (1)$$

Consequently, supposing that the distance between the center of the bubble and the probe tip follows a uniform distribution, the radius and the bubble velocity vector being known, the probability density function of the distance between the center of the bubble and the probe tip is as follows

$$P_r(r/R, \theta, \phi) = \frac{2r}{R^2 \frac{(\alpha \cdot \tan \theta)^2 + 1}{(\alpha \cdot \tan \theta \cdot \sin \phi)^2 + 1}}; \quad r \in \left(0, R \sqrt{\frac{(\alpha \cdot \tan \theta)^2 + 1}{(\alpha \cdot \tan \theta \cdot \sin \theta)^2 + 1}}\right) \quad (2)$$

Knowing the radius, the distance of the probe to the center of the bubble, and the direction of the velocity vector, the chord length y measured by the probe when a bubble goes through it will be

$$y = 2\alpha \sqrt{\frac{\tan^2 \theta + 1}{(\alpha \cdot \tan \theta)^2 + 1}} \left(R^2 - r^2 \frac{(\alpha \cdot \tan \theta \cdot \sin \theta)^2 + 1}{(\alpha \cdot \tan \theta)^2 + 1} \right) \quad (3)$$

and how

$$P_y(y/R, \theta, \phi) = P_r(r/R, \theta, \phi) \cdot \left| \frac{dr}{dy} \right| \quad (4)$$

Once the chord length distribution measured by the probe is known, the velocity vector and the bubble radius is given by

$$P_y(y/R, \theta, \phi) = \frac{y}{2R^2\alpha^2} t^2(\theta); \quad y \in \left(0, \frac{2R\alpha}{t(\theta)}\right) \quad (5)$$

where

$$t^2(\theta) = \frac{(\alpha \cdot \tan \theta)^2 + 1}{\tan^2 \theta + 1} \quad (6)$$

From Eq. 5, it is important to take into account that if the bubble radius R and the zenith angle θ are independent of the azimuth angle ϕ , the chord length y will also be independent. The possible dependence of y on ϕ depends on R or θ , as it is observed in Eq. 5.

Using the total probability theorem to determine the probability of the chord length measured by the probe depending on the direction of the velocity vector and independent of the bubble radius, we can get

$$P_y(y/\theta, \phi) = \int_{\frac{y}{2\alpha}}^{\infty} \frac{y}{2R^2\alpha^2} \cdot t^2(\theta) \cdot P_R(R/\theta, \phi) \cdot dR \quad (7)$$

Deriving the previous equation with regard to the chord length measured by the probe

$$y \cdot P_y'(y/\theta, \phi) = \int_{\frac{y}{2\alpha}}^{\infty} \frac{y}{2R^2\alpha^2} \cdot t^2(\theta) \cdot P_R(R/\theta, \phi) \cdot dR - \frac{t(\theta)}{\alpha} \cdot P_R\left(\frac{y}{2\alpha} t(\theta)/\theta, \phi\right) \quad (8)$$

and substituting Eq. 7 in Eq. 8, the analytic backward transform is obtained, which relates the bubble-size distribution and the chord length measured by the probe, the bubble direction being known, so that

$$P_R\left(\frac{y}{2\alpha} t(\theta)/\theta, \phi\right) = \frac{\alpha}{t(\theta)} \cdot [P_y(y/\theta, \phi) - y \cdot P_y'(y/\theta, \phi)] \quad (9)$$

With the following variable change in the previous equation, where we attribute the bubble-size distribution to be the distribution implied by the largest chord lengths corresponding to each bubble size and each rise angle, we get

$$R = \frac{y}{2\alpha} \cdot t(\theta) = \frac{y}{2\alpha} \sqrt{\frac{(\alpha \cdot \tan \theta)^2 + 1}{\tan^2 \theta + 1}} \quad (10)$$

Obtaining the way to determine the bubble-size distribution from the chord length read by the probe, the bubble attach angle being known, we get

$$P_R(R/\theta, \phi) = \frac{\alpha}{t(\theta)} \cdot \left[P_y\left(\frac{2R\alpha}{t(\theta)} \middle/ \theta, \phi\right) - \frac{2R\alpha}{t(\theta)} \cdot P_y\left(\frac{2R\alpha}{t(\theta)} \middle/ \theta, \phi\right) \right] \quad (11)$$

Finally, using the total probability theorem again, the probability density function of bubble sizes is obtained, which is a generalization of bubbles with a nonvertical rise of the analytic backward transform obtained by Liu and Clark (1995) for bubbles with a purely vertical rise

$$P_R(R) = \int_{\phi} \int_{\theta} \frac{\alpha}{t(\theta)} \cdot \left[P_y\left(\frac{2R\alpha}{t(\theta)} \middle/ \theta, \phi\right) - \frac{2R\alpha}{t(\theta)} \cdot P_y\left(\frac{2R\alpha}{t(\theta)} \middle/ \theta, \phi\right) \right] \cdot P_{\theta, \phi}(\theta, \phi) d\theta d\phi \quad (12)$$

If we assume that the bubble radius R and the zenith angle θ are of the Azimuth angle ϕ , as well as the chord length y , that is, if we hypothesize that bubble-size distribution is independent of the horizontal rotations, the bubbles, Eq. 12 will be transformed into

$$P_R(R) = \int_{\theta} \frac{\alpha}{t(\theta)} \cdot \left[P_y\left(\frac{2R\alpha}{t(\theta)} \middle/ \theta\right) - \frac{2R\alpha}{t(\theta)} \cdot P_y\left(\frac{2R\alpha}{t(\theta)} \middle/ \theta\right) \right] \cdot P_{\theta}(\theta) d\theta \quad (13)$$

Therefore, in order to know the local distribution of bubble sizes, we have to know the conditional probability density function for a chord length $P_y(y/\theta)$ and the distributions of bubble directions $P_{\theta}(\theta)$.

Finally, it is necessary to mention that this new method for transforming chord-length data to a local bubble-size distribution independent of the direction of the velocity vector presented herein is preferable to other literature because there is no restriction for the rise angle of the bubbles. Also, it more realistically represents the actual bubble-size distribution in a fluidized bed.

Parzen's Window

The problem to determine the density function from a sample of data can be seen from two different techniques: The parametric and the nonparametric one.

The first one, taking a density function *a priori* tries to determine the parameters which better fix the aprioristic density function from the samples.

The second one, the nonparametric technique, does not need to fix any density function *a priori*. Therefore, it is much

more suitable than the parametric one when there is no previous information about the density functions of the sample points. That is the case of the distributions of the chord lengths measured by the probes. A study of different non-parametric techniques described in full detail can be found in the work of Johnston and Kramer (1994).

The nonparametric method used to fix the density function from the sample will be the technique developed by Parzen (1962). Let (x_1, x_2, \dots, x_n) be independent and identically distributed random variables according to the density function $P(x)$, then

$$\lim_{n \rightarrow \infty} E[P_n(x)] = P(x) \quad (14)$$

$$P_n(x) = \frac{1}{n \cdot h} \sum_{i=1}^n K\left(\frac{x - x_i}{h}\right) \quad (15)$$

and $K(\cdot)$ a weighting function and $\lim_{n \rightarrow \infty} h(n) = 0$, where h is known as the Parzen window width.

After that, we can use an asymptotically unbiased estimator of the function $P(x)$ for each point of continuity x from x_1, x_2, \dots, x_n (samples), and we do not have to fix a density function *a priori*.

The previous result is applied to our problem. With (y_1, y_2, \dots, y_n) being a set of chord-length data measured by the probe, and once the bubble attack angle is known and fixed as well as taken as the weighting function,

$$K(x) = \frac{1}{\sqrt{2\pi}} \exp\left(-\frac{1}{2}x^2\right) \quad (16)$$

$$P_n(y/\theta, \phi) = \frac{1}{n \cdot h} \sum_{i=1}^n \frac{1}{\sqrt{2\pi}} \exp\left(-\frac{1}{2}\left(\frac{y - y_i}{h}\right)^2\right) \quad (17)$$

it is an asymptotically unbiased estimator for any point of continuity of the density function of chord length given the bubble attack angle.

If we also suppose that the density function of the chord-lengths measured by the probe and the weighting function are derivable, then the derivative of Eq. 17 is an asymptotically unbiased estimator of the derivative of the density function for any point of continuity of the derivative.

Replacing the chord length distribution estimator (Eq. 17) by the density function in Eq. 9 and changing the variable, we get an asymptotically unbiased estimator of the local bubble radii given the attach angle

$$P_n(R/\theta, \phi) = \frac{\alpha}{t(\theta)} \frac{1}{nh} \frac{1}{\sqrt{2\pi}} \left[\sum_{i=1}^n \left(1 + \frac{2R\alpha}{t(\theta)} \left(\frac{2R\alpha}{t(\theta)} - y_i \right) \right) \exp\left(-\frac{1}{2}\left(\frac{\frac{2R\alpha}{t(\theta)} - y_i}{h}\right)^2\right) \right] \quad (18)$$

It is important to take into account that the previous equation fulfills the properties of probability functions. The integral along the real straight line is one, and it is not negative if a suitable choice of the Parzen window width h is made because, when the sample is fixed, the sign of the previous equation depends on the choice of the Parzen window width.

Then, the problem we have to define with Eq. 20 is to determine Parzen window width given a sample of chord-lengths measured by the probe given the attack angle.

Fixing of Parzen Window Width

The fixing of h is a problem to be treated carefully because an overestimation produces a flat density function, and an underestimation produces irregular distributions.

The measure of performance used to get an optimum h from which we get the estimator that better fixes the density function, is the measure used by Traven (1991), the probability product of sample points which are chosen in an aleatory way.

Then, the problem that arises is to determine h so

$$J = \sum_{i=1}^{n_{\text{test}}} \log(P_n(y_i/\theta_j)) \quad (19)$$

it is maximum.

For fixing the window width, the method of crossed validation described by Weiss and Kulikowski (1991) will be used, because such a method uses all the sample points in the determination of the estimator.

Therefore, it is necessary to carry out the following steps:

- (1) Divide the whole of data into a n_{test} subset of n/n_{test} sample points;
- (2) Fix, h ;
- (3) Calculate J (Eq. 19) taking the first subset as a subset to be validated and the other used to build the density function estimation;
- (4) Repeat the third step using each subset to be validated;
- (5) Calculate the sum of J for all of the subset; and
- (6) Return to the second step with another h and repeat the process till an optimum h may be obtained.

After that, to calculate h , we will follow the previous method provided that the radii density value is positive.

The previous process will have to be repeated for the different angles in which Eq. 13 is found discretized (in the present simulation, an increase of one degree is chosen), and later with the densities function previously calculated, we can infer the local bubble-size distribution

$$P_n(R) = \sum_{j=0}^n P_n(y/\theta_j) \cdot P(\theta_j) \quad (20)$$

The only case where the discretization is not necessary to infer bubble-size distribution is the case in which the shape of the bubble is spherical, because its determination may be directly attacked by using Eq. 13:

Bingham's Distribution

When we want to determine both magnitudes and directions of the random vectors, we have to examine thoroughly the field of analysis of directional data. A precise reference of this type of analysis may be found in Mardia et al. (1979). In the present simulation, the two dimensional Bingham distribution has been chosen

$$B(\theta; \theta_m, k) = \exp [k \cdot \cos(2(\theta - \theta_m))] / [2 \cdot \pi \cdot I_0(k)],$$

$$k > 0, 0 \leq \theta < 2\pi \quad (21)$$

where k is the concentration parameter, θ_m is the mean angle, and $I_0(k)$ is the modified Bessel function of the first kind and order zero.

In Figure 2, we can observe the effect of the concentration parameter k for a mean angle of 0° . The figure also shows that if the concentration parameter increases, the probability function $P(\theta)$ concentrates around the mean angle. Obviously, for $k = 0$, we had a uniform distribution, while for $k = 100$ we had a distribution where the probability of the angle is between $\pm 10^\circ$; it is 99%, which is to be expected.

It is important to take into account that if the representation is done for the total of angles of the circumference, the representation will be a figure similar to the previous one (Figure 2), but with a bimodal distribution with modes being separated 180° . For this reason, Bingham's distribution is also called Von Mises bimodal distribution (Mardia, 1972).

In our case, we have supposed a distribution of bubble rise angles, knowing the radius R in such a way that the probability function verifies the following properties: The probability that the bubble rise is vertical increases with the bubble diameter due to the effects of the bed wall and the interaction between bubbles.

Therefore, a variation with the radius of the concentration parameter and a mean rise angle of 0° have been chosen, so that $P_\theta(\theta/R) = B(0^\circ, k(R))$ and

$$k(R) = F_R(R) \cdot 100 \quad (22)$$

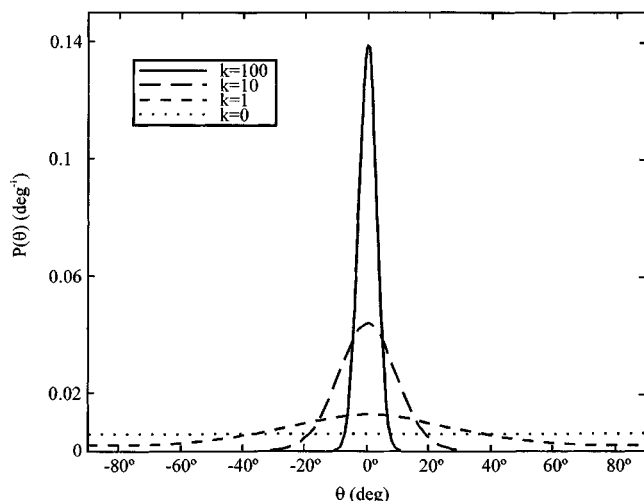


Figure 2. Effect of the concentration parameter on the Bingham distribution.

where $F_R(R) \equiv P_R(R < R)$ is the function of the bubble-size distribution in such a way that the concentration parameter is around 100 for bubbles whose radius is over 99% of the distribution of bubble radii.

It is obvious that the choice of the concentration parameter is in a way arbitrary, because there are no experimental data of the dependence of the radius with the rise angle. However, this approach is valid because our goal is to see the difference between the estimation of local bubble-size distribution with vertical rise and the local bubble-size distribution with any attack angle.

Simulation Process

The process of simulation of the chord length read by the probe allows us to interpret the local bubble-size distribution, when chord length data and the bubble shape factor α are known. Several sets of 5,000 chord lengths were generated synthetically for the ellipsoidally-shaped bubble model using the Monte-Carlo method to simulate the sample points of Bingham's distribution and the limit central theorem for the log-normal distribution.

The simulations were realized fixing the shape factor ($\alpha = 0.6$). These chord lengths were discretized in terms of the rise angle, and we have chosen an increase of 1° . In this way, with each sample whole of chord lengths, we can estimate every conditional probability density function and, from these, we can determine the local bubble-size density distribution.

Simulations were conducted based on the following steps:

(1) Simulate R according to the distribution of $P_R(R)$; in the present example we have used a log-normal (2.8, 0.3).

(2) Given R simulate $P_\theta(\theta/R)$ following a Bingham distribution with a mean vertical rise ($\theta_m = 0$) and concentration parameter $k(R)$.

(3) Simulate ϕ following a uniform distribution in $(0, 2\pi)$, because it has been supposed that ϕ is independent of R and θ .

(4) Determine the chord length y according to Eq. 3 fixing the shape factor α .

With this new method, we get the chord length sample measure by the probe for each rise angle of the bubbles, because we have considered that the bubbles follow an intricate pattern and bubble orientation and rise velocity may not be vertical. Finally, from this chord length distribution we can get the local bubble-size distribution by using any rise angle.

Result and Discussion

Figure 3 shows the local bubble-size density distribution as a function of the rise angle of the bubbles varying with bubble sizes and, knowing the radii for several different rise angles, the size density distribution can be observed. The simulation was made with 5,000 bubbles of a known size distribution, all with the same shape factor ($\alpha = 0.6$). Those figures show that the conditional probability density function $P_\theta(R/\theta)$ for several rise angles varies with bubble sizes, and, if the bubble sizes increase to a specific value, then a great probability exists that the rise angle approaches significantly to the vertical.

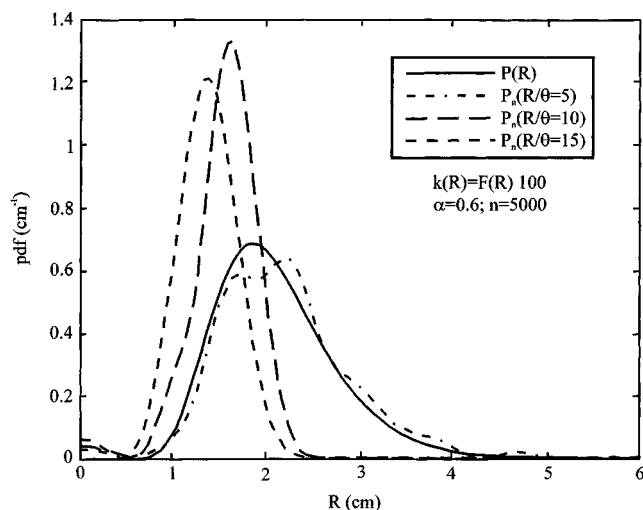


Figure 3. Local bubble-size density distribution as a function of the rise angle of the bubbles.

As the rise angle was increased, the conditional probability density function became smooth and was closer to the left side of Figure 3. This illustrates that when the bubble sizes decrease, the probability of the rise angle deviates significantly from the vertical increases, because the bubble shape is dynamic and exits interaction with other bubbles in the vicinity, as well as the local solid flow and wall of the fluidized bed.

Figure 4 shows the rise angle density distribution of the bubbles $P_n(\theta)$ and the Bingham distribution $B(\cdot)$, as a function of the rise angle distribution of the bubbles $P(\theta)$ with the rise angles. It can be observed that $P_n(\theta)$ can be conveniently represented by a Bingham distribution with a mean corresponding to vertical bubble rise ($\theta = 0^\circ$) and a concentration factor of 37.

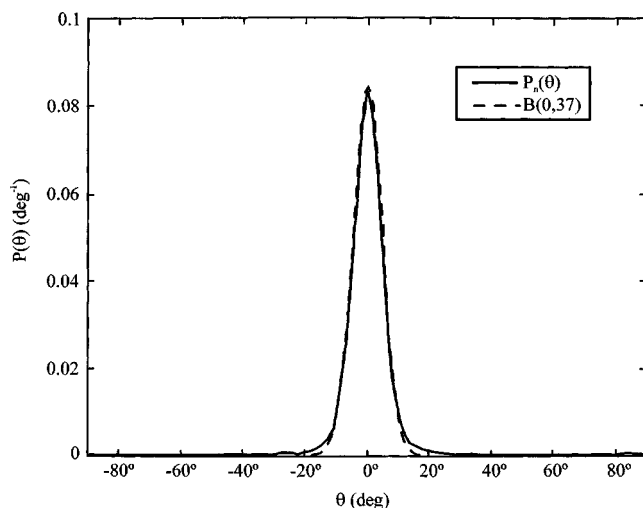


Figure 4. Rise angle density distribution of the bubbles and the Bingham distribution.

This result ($\theta_m = 0^\circ$) is in agreement with the limited experimental data given by Gunn and Al-Doori (1985) and plotted by Lim and Agarwal (1992), where these authors used a normal density function with a mean corresponding to a vertical bubble rise ($\theta = 0^\circ$) and a standard deviation of 14° , so that it is a Bingham Distribution with a mean angle of 0° and a concentration parameter of 4.5.

Figure 4 illustrates that the optimal estimate $P_n(\theta)$ is closer to the Bingham Distribution $B(0, 37)$; then the error in the prediction of the local bubble-size density distribution depends on the rise angle which is related to the radius of the bubble. This error is not due to the selection of a few bubble sample sizes, because, in our simulation, we have used 1,000 bubble sample sizes with vertical rise.

Figure 5 shows the best estimates of the local bubble-size density distribution for the 5,000 bubble samples with a shape factor $\alpha = 0.6$ and the original distribution.

Monte-Carlo simulation was used to generate ellipsoidally-shaped bubbles with several rise angles, around an imaginary probe based on the fact that the size density distribution of bubbles affecting the probe was the Bingham Distribution $B(0^\circ, k(R))$, which is represented by Eq. 22 with $k(R) = F(R) 100$.

As can be seen in the four simulations in Figure 5, the transformation of chord length data obtained by probes using the Parzen window as an estimator of the probability density functions gives a good estimation of the local bubble-size distribution $P(R)$ for different rise angles.

For comparison of the set of simulation in Figure 5, it can be observed that the simulation is not perfect because the Monte-Carlo method is a probabilistic simulation, and the chord length data are therefore generated randomly and it cannot be expected to be the same as the theoretical continuous distribution.

It can be observed that the best global estimation of the local bubble-size distribution $P_n(R)$ is the Parzen window estimator for bubbles with any rise angle. This is due to the dependence between size and angle supposed, but an error will be made when inferring the local bubble-size distribution from a distribution of bubbles with vertical rise only. In this case, for the same set of samples, the local bubble-size distribution with vertical rise $P_n(R/\theta = 0)$ becomes wide and the cumulative error increases, as shown in Figure 5.

The mean quadratic error between the estimates $P_n(R)$ and $P_n(R/\theta = 0)$ and the original value of $P(R)$ for all the sample points, defined as

$$MQE = \sum_{i=1}^n (P(R_i) - P_n(R_i))^2 / n$$

$$MQE_0 = \sum_{i=1}^{n_0} (P(R_i) - P_n(R_i/\theta = 0))^2 / n_0 \quad (23)$$

was calculated.

The mean quadratic error for the simulations of Figure 5 vary for each run; it can be observed that the error was between 0.005 and 0.0044 for $P_n(R)$ and 0.0153 to 0.0238 for the local bubble-size distribution with vertical rise $P_n(R/\theta =$

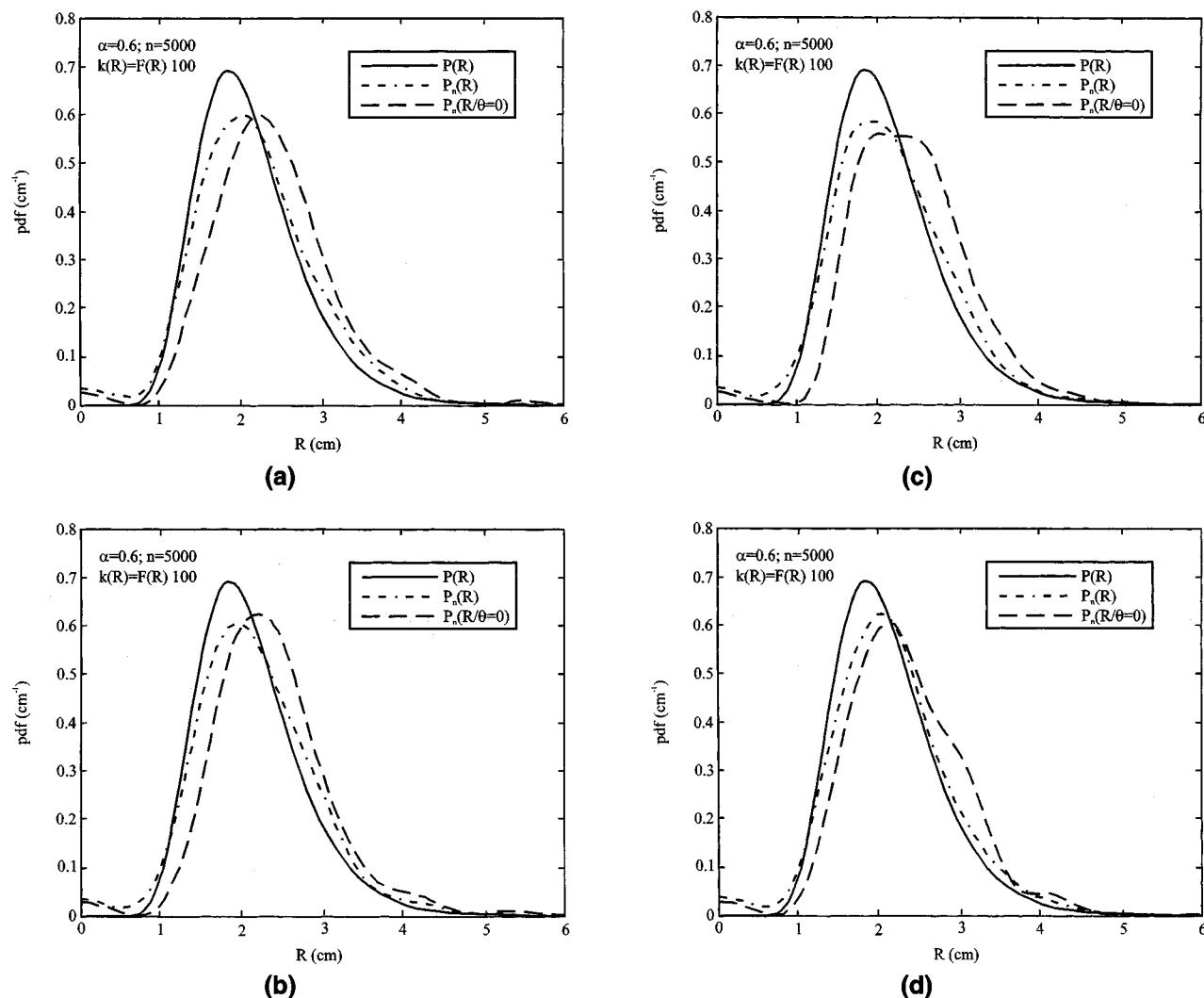


Figure 5. Best estimates of the local bubble-size density distribution for the 5,000 bubbles samples and the original distribution.

0). The accuracy of this approach (local bubble-size distribution with any rise angle) was therefore satisfactory and the superior agreement given in Figure 5 is evident.

The new method for transforming chord length data to local bubble-size distribution for any direction of the velocity vector for any orientation of the bubble, or if the rise angle deviates significantly from the vertical, gives a superior agreement than the approach where the bubble-size distribution is determined from bubbles with vertical rise.

This suggests that the distribution of bubbles with vertical rise $P_n(R/\theta = 0)$ underestimates the smaller bubbles and overestimates the bigger ones. On the other hand, it is important to point out that similar results have been obtained by Santana (1999) for other models of bubbles (spherical cap) and it was found that the local bubbles-size distribution determined with vertical rise of the bubbles has a larger cumulative square error between the estimates $P_n(R/\theta = 0)$. Also, the original distribution $P(R)$ and the new approach offered in this article is more feasible, effective, and accurate for in-

ferring local bubble-size distribution from chord length data directly in a fluidized bed.

Conclusions

A method for transforming chord-length distribution to local bubble-size distribution knowing the direction of velocity vectors has been proposed, using the Parzen window as an estimator of the probability density functions.

Monte-Carlo simulation was used to generate bubbles synthetically with several rise angles in a fluidized bed, based on the fact that the ascent angle density distribution of bubbles was a Bingham distribution.

The new approach demonstrates that the local size distribution, knowing the direction of the velocity vector for any rise angle of the bubble, has a superior agreement with the theoretical distribution.

The new approach offered in this article is the most general form for transforming the chord-length distribution from

bubbles with any rise angle to local bubble-size distribution for ellipsoidally shaped bubbles.

The new approach offered in this article is more feasible, effective, and accurate for inferring local bubble-size distribution from chord length data directly. It is preferable to other literature, because it more realistically represents the actual bubble-size distribution in a fluidized bed.

Acknowledgments

The financial support from CICYT of the Spanish Government is appreciated (Project number AMB95-0200). We would also like to acknowledge the assistance of Dr. Daniel Fyfe, who helped us with the editing of our written results.

Notation

- $F_R(\cdot)$ = R distribution function
 $I_0(\cdot)$ = modified Bessel function of the first kind and order 0
 J = logarithmic of the probability product
 MQE = mean quadratic error
 MQE₀ = mean quadratic error for bubbles with vertical ascent
 n = number of bubbles
 n_0 = number of bubbles with vertical ascent
 $P(\cdot)$ = probability density function
 $P_n(\cdot)$ = Parzen window estimation
 $P_{\theta,\phi}(\theta, \phi)$ = probability density function of the bubble velocity vector direction
 $P_R(R/\theta, \phi)$ = probability density function of the bubble radius, knowing the velocity vector direction
 $P_r(r/R, \theta, \phi)$ = probability density function of the distance between the bubble center and the probe tip, knowing the velocity vector direction and bubble radius.
 $P_y(y/R, \theta, \phi)$ = probability density function of the chord length, knowing the velocity vector direction and bubble radius
 r_{\max} = maximum distance between the bubble center and the probe tip knowing the shape, velocity vector direction and bubble radius.
 $f(\theta)$ = function defined in Eq. 6
 x = aleatory variable
 x_i = sample point of the x aleatory variable

Literature Cited

- Cheremisinoff, N. P., "Review of Experimental Methods for Studying the Hydrodynamics of Gas-Solid Fluidized Beds," *Ind. Eng. Chem. Process Res. Dev.*, **25**, 329 (1986).
 Clark, N. N., W. Liu, and A. I. Karamavruc, "Data Interpretation Techniques for Inferring Bubble Size Distribution from Probe Signals in Fluidized Systems," *Powder Technol.*, **88**, 179 (1996).

- Feller, W., *An Introduction to Probability Theory and its Applications*, Wiley, New York (1978).
 Gunn, D. J., and H. H. Al-Doori, "The Measurement of Bubble Flow in Fluidized Beds by Electrical Probe," *Int. J. Multiphase Flow*, **11**, 535 (1985).
 Henríquez, V., A. Lozano, and A. Macías-Machín, "Influence of a Decanting-Mixing Chamber in Aerosol Generation," *Proc. I. International Symp. on Filtration and Separation*, Salamanca, Spain, 98 (1995).
 Johnston, L. P. M., and M. A. Kramer, "Probability Density Estimation using Elliptical Basis Function," *AIChE J.*, **40**, 1639 (1994).
 Lim, K. S., and P. K. Agarwal, "Bubble Velocity in Fluidized Beds: The Effect of Non-Vertical Bubble Rise on its Measurement Using Submersible Probes and its Relationship with Bubble Size," *Powder Technol.*, **69**, 239 (1992).
 Liu, W., and N. N. Clark, "Relationships Between Distributions of Chord Lengths and Distributions of Bubble Size Including their Statistical Parameters," *Int. J. Multiphase Flow*, **21**, 1073 (1995).
 Liu, W., N. N. Clark, and A. I. Karamavruc, "General Method for the Transformation of Chord-Length Data to a Local Bubble Size Distribution," *AIChE J.*, **42**, 2713 (1996).
 Mardia, K. V., J. T. Kent, and J. M. Bibby, *Multivariate Analysis*, Academic Press, London (1979).
 Mardia, K. V., *Statistics of Directional Data*, Academic Press, London (1972).
 Parzen, E., "On Estimation of a Probability Density Function and Mode," *Ann. Math. Stat.*, **33**, 1065 (1962).
 Santana, D., J. M. Rodríguez, and A. Macías-Machín, "Modelling Fluidized Bed Elutriation of Fine Particles," *Powder Technol.*, **106**, 110 (1999).
 Santana, D., PhD Diss., Universidad de Las Palmas de Gran Canaria, Canary Islands, Spain (1999).
 Traven, H. G. C., "A Neural Network Approach to Statistical Pattern Classification by Seimparametric Estimation of Probability Density Function," *IEEE Trans. Neural Networks*, **NN-2**, 366 (1991).
 Turton, R., and N. N. Clark, "Interpreting Probe Signals from Fluidized Beds," *Powder Technol.*, **59**, 117 (1989).
 Venkata Ramayya, A., S. P. Venkateshan, and Ajit Kumar Kolar, "Bubble Detection with Horizontal Pressure Gradient Measurements in Gas-Fluidised Beds," *Powder Technol.*, **97**, 77 (1998).
 Venkata Ramayya, A., S. P. Venkateshan, and Ajit Kumar Kolar, "Estimation of Bubble Parameters from Differential Pressure Measurements in Gas-Fluidized Beds," *Powder Technol.*, **87**, 113 (1996).
 Weiss, S. M., and C. A. Kulikowski, *Computer Systems that Learn*, Morgan-Kaufman, San Mateo, (1991).
 Werther, J., "Bubble in Gas Fluidised Beds-Part I," *Trans. Inst. Chem. Engrs.*, **52**, 149 (1974).
 Werther, J., "Bubbles in Gas Fluidised Beds-Part II," *Trans. Inst. Chem. Engrs.*, **52**, 160 (1974).

Manuscript received Dec. 21, 1999.